Section 5

XRCF and the HETG

5.1 XRCF Harware Introduction

During December 1996 through April 1997 all three key components of the HETGS, HRMA-HETG-ACIS-S, were integrated for test at NASA's Marshall Space Flight Center (MSFC) in their X-Ray Calibration Facility (XRCF). The XRCF and related hardware are described in great depth in the documents listed in Table 5.1, however some key concepts are presented here for completeness and to support the grating analysis discussion.

Table 5.1: XRCF Documents and References

XRCF Phase 1 Testing: Preliminary Results	MST	June 1997
Calibration of the AXAF: Project Science Analyses	Weisskopf *et al.*	October 1997

The general layout of XRCF hardware is shown in Figures 5.1 and 5.2 and specifics of the key subsystems are presented in the sections below.

Calibration was divided into two main calibration phases, Phase 1 and Phase 2, defined physically by differences in the focal plane detectors; the Beam normalization detectors (BND) were present in both Phases. Each of these major phases had subphases designated sequentially by letter, see Table 5.2.

In Phase 1 the non-flight detectors, FPC_X2 (Flow Proportional Counter), SSD_X (Solid State Detector), and HSI (micro-channel plate High Speed Imager), were in the focal plane. The philosophy of Phase 1 is that the detectors are (or will be) well characterized and of proven and understood technology so that measurements are performed to understand the HRMA and gratings. Grating-in grating-out measurements were performed to measure grating Efficiency; images and scans were obtained to verify the grating LRF model.

In Phase 2 a "two-chip ACIS" (ACIS-2C) and the flight ACIS and HRC detectors were variously present. Here the philosophy is that the HRMA and gratings are understood and the flight detectors and/or the HRMA-(grating-)detector interaction is being studied. For this reason, the HETG tests were primarily related to Effective Area. Because LRF tests generally require well focussed beams and given the HRC pore extraction limits and the ACIS telemetry limits,

Table 5.2: XRCF Phases and Detectors

Phase	Desig.	Focal Plane	Comments
Rehearsal 1	A	FPC, SSD, HSI	TMA and TOGA
Rehearsal 2	B	FPC, SSD, HSI	"
Phase 1.1	C	FPC, SSD, HSI	HXDA translation system
Phase 1.2	D	FPC, SSD, HSI	"
Phase 1.3	E	FPC, SSD, HSI	"
Phase 2.1	F	ACIS-2C	detector on FAM
Phase 2.2	G	HRC and '2C	"
Phase 2.3	H	ACIS	"
Cross-cal 1	I	ACIS	Flat fields, no HRMA
Cross-cal 2	J	FPC, SSD, HSI	HXDS detector cross-calibrations

extensive LRF studies were not in general carried out with the HETG in Phase 2 – the exception being enough data with ACIS-S to allow us to verify the Rowland curvature of the CCDs.

5.1.1 XSS

Details of the X-Ray Source System (XSS) are presented in Kolodziejczak *et al.* [42].

5.1.2 Double Crystal Monochromator (DCM)

The DCM is part of the X-ray Source System (XSS) used at XRCF [74, 42]. It offered three 3 different crystals for these tests, of which we only used the Thallium Acis Phthlate (TAP) between 0.9 and 2.5 keV and the germanium (Ge111) between 2.5 and 8.7 keV. The source is a rotating-anode tungsten source, which operates at a high voltage to generate a strong continuum, however it also produces several bright W lines at 1.38, 1.78, and 1.84 keV. Those lines actually proved quite useful for tests of HETG scattering, Sections 6.6 and 3.3. The DCM has an energy gradient in dispersion direction, which results in a non-negligible beam non-uniformity when tuned near the the W lines. Another source of non-uniformity is introduced while using the TAP crystal due to some waviness on the crystals surface.

5.1.3 BNDs

The beam normalization detectors (BNDs) monitor the source flux without the effects of the HRMA or HETG. There are six BND detectors: two, a Flow Proportional Counter (FPC) and a Ge solid state detector (SSD), are located 37.43 and 38.20 meters from the source in "Building 500", and four FPCs surround the HRMA entrance, see Figure 5.2. To ensure some BND data is available over a wide range of source flux, apertures can be selected on the FPC_5, SSD_5, and FPC_HN BNDs.

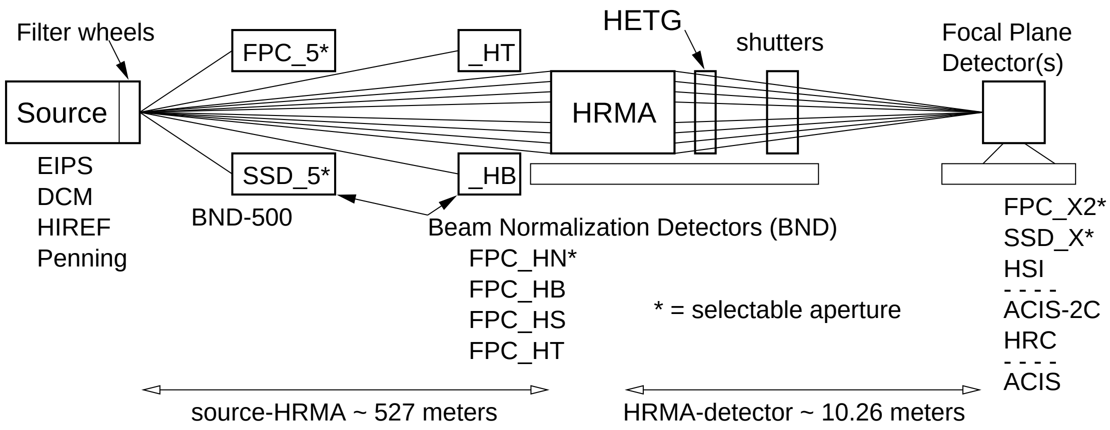

Figure 5.1: XRCF hardware schematic. The XRCF HETG configurations include i) X-ray source and filters, ii) Beam normalization detectors (BNDs), iii) AXAF optics (HRMA, HETG), iv) shutter assembly, and v) focal plane detectors.

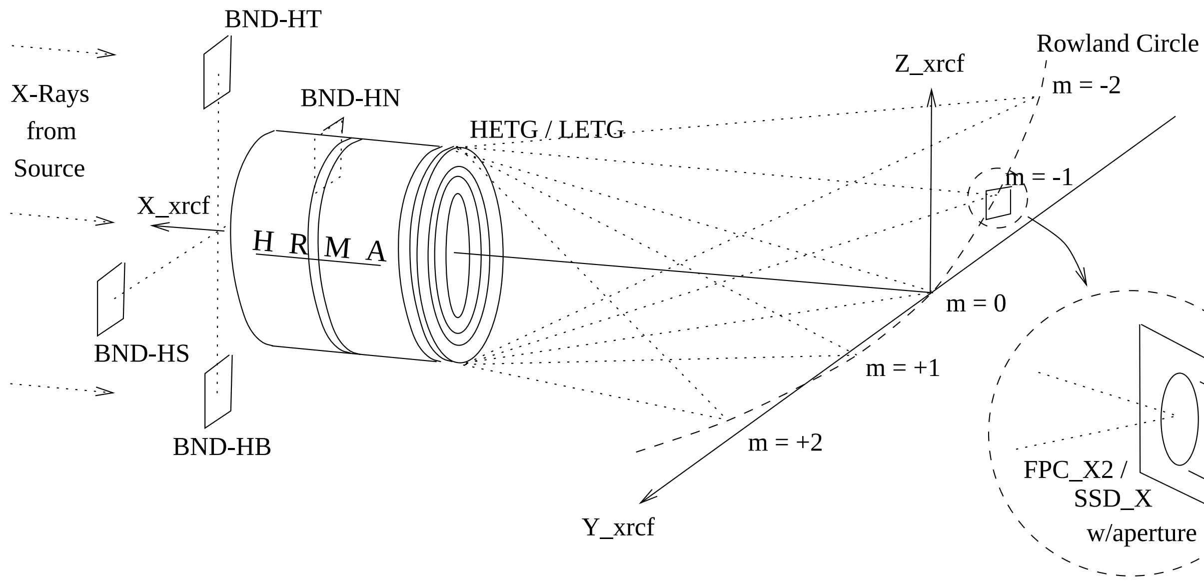

Figure 5.2: Phase 1 Hardware Schematic. In all phases the incident source flux is monitored by a set of beam monitor detectors (BNDs), four of which are located around the HRMA entrance aperture, shown at left. One or the other of the AXAF gratings, HETG or LETG, may be inserted into the converging HRMA beam. The HXDS detectors, of similar design to the BNDs, are located in the focal plane and can be positioned through 3-axes of motorized stages. For example, the FPC with aperture can be moved along the curved, inclined HEG Rowland circle (dashed curve) in order to intercept the diffracted beam.

5.1.4 HRMA, Gratings, and Shutters

The HRMA, gratings and shutters were all mounted to a common platform at XRCF. The status of the shutters was recorded in a shutter log with the format:

```
   Shell       1     3     4     6
 quadrant    tnbs  tnbs  tnbs  tnbs
             cccc  ooeo  cccc  cccc
```

where the letter codes corespond to “open”, “closed”, and “error”.

Some useful XRCF HETG parameters are tabulated in Table 5.3 for reference.

Table 5.3: Table of useful XRCF HETG parameters. These preliminary values are based on sub-assembly and XRCF testing, from Calibration Products, Section 9.3.

Description	value	error	units	comments
Rowland distance	8782.8	0.5	mm	see Section 5.2.1
MEG average period	4001.41	≈ 0.10	Å	based on lab measurement
HEG average period	2000.81	≈ 0.05	Å	LR/NIST: based on lab measurement
MEG angle	4.74	0.05	deg.s	
HEG angle	-5.19	0.05	deg.s	
MEG-HEG angle	9.934	0.008	deg.s	
(MEG+HEG)/2 angle	-0.225	0.01	deg.s	(-0.275 in Phase C)

5.1.5 HXDS Focal Plane System

In Phase 1 the non-flight detectors, FPC_X2 (Flow Proportional Counter), SSD_X (Solid State Detector), and HSI (micro-channel plate High Speed Imager), were in the focal plane.

5.1.5.1 HXDS Axes

The HXDS axes are nominally along the XRCF coordinates, Figure 5.2. The HXDS primeY axis, however, was determined after-the-fact to have had its axis rotated by an angle of 0.0058 radians about $+Z_{\rm xrcf}$. Thus a commanded motion in the $+Y_{\rm xrcf}$ direction resulted as well in a motion of $0.0058 \times \Delta Y$ in the $-X_{\rm xrcf}$ direction. **MARX** simulations of XRCF measurements must take this into account.

5.1.5.2 HSI in the Focal Plane

During Phase 1 calibration the HSI detector[21] provided imaging capability at high event rates, for example the image in Figure 1.6. The HSI also was fitted with a mask with a “cusp” to allow the bright PSF core to be occulted while the surrounding wings of the PSF were observed.

5.1.5.3 FPC and SSD in the Focal Plane

The FPC and SSD are non-imaging detectors with moderate energy resolution and have a variety of apertures used to isolate and measure grating-dispersed spectral features in the focal plane, *e.g.*, the aperture of diameter D in Figure 5.2. These detectors have well studied characteristics[77, 51], are similar to the BNDs, and provide some of the fundamental data for characterizing the efficiencies and effective area of the system without the novelty and complication of the flight-detectors and their $QE(E, \dots)$ terms.

The FPC and SSD detectors could have a slit aperture selected for use - in this way a direct measurement of the 1D LRF was possible, Section 6.3

5.1.6 ACIS-2C

Extensive LRF tests could be performed with the ACIS-2C detector given its (non-flight) high event-rate readout.

5.1.7 ACIS

ACIS was installed in XRCF with its $+Z$ axis pointing in the $-Z_{\rm xrcf}$ direction.

5.1.8 HRC

5.2 Differences between XRCF and Flight

The arrangement and operation of the components at XRCF are flight-like with the following differences:

○ The source is not infinitely far away and so i) the HRMA focal length is greater than the flight value and ii) the HRMA reflection angles and optic illumination are different from flight.
○ The HRMA is in a "1-g off-loaded" condition approximating the 0-g flight configuration, so flight PSFs will be slightly different.
○ The $+Z$ axis of the HRMA, gratings, and flight detectors pointed "down" at XRCF, (*i.e.*, aligned to XRCF $-Z$).
○ The gratings are designed to operate at a Rowland distance of 8633.69 mm but because of the HRMA focal length change they are placed $\approx$ 8800 mm from the focus; this introduces negligible LRF effects and some slight additional vignetting, primarily for the LETG ($< 5\%$).

5.2.1 HETG Location at XRCF

The Rowland spacing of the grating is the on-axis Rowland circle intercept to focal plane distance. This spacing must be inferred from measurements between the HETG and HRMA as well as assumed/measured location of the HRMA focus w.r.t. the HRMA fiducial location, *e.g.*, CAP center line.

In order to put measured values into context it is important to have various axial reference points of the HRMA and gratings well defined and specified relative to each other; these references are tabulated in Table 5.2.1.

HETG Axial References	X_g
$X_g = 0$	0.0
HESS/GESS surface (metrology reference)	0.800 inches
ARM reflective surface	1.500 inches
OTG Datum -D- alignment pad surface	1.670 inches
Rowland intercept	2.500 inches
HRMA Axial References	**X w.r.t. CAP CL**
CAP CL (midplane)	0.0
HRMA node	0.371 inches
CAP Datum -A-	0.9825 inches
XRCF ARM	2.846 inches

Table 5.4: Axial references for HETG and HRMA.

The following equation gives the Rowland spacing in terms of other measurable values:

$$\text{(RC spacing)} = \text{(Focus to CAP CL)} \; - \; \text{(CAP CL to OTGorg)} \; + \; \text{(OTGorg to RC)} \tag{5.1}$$

Values for these quantities are tabulated, Table 5.2.1, for three cases:

- (i) XRCF design drawing (301331)

- (ii) drawing plus a 0.392 inch shim designed to improve the vignetting performance of the gratings designed to improve the vignetting performance of the gratings
- (iii) post-XRCF values inferred from HRMA ARM to OTG ARM laser ranger measurements and improved HRMA focal length value

The later of these is TRW's best value for the as-used spacing at XRCF. The error on the Rowland Spacing at XRCF is at least 0.5 mm due to error in determining the "Focus to CAP CL" distance. Additionally, the "CAP CL to OTGorigin" distances were measured with a laser ranger, measuring the distance between the grating ARM reflective surface and the HRMA "XRCF ARM" surface. This measurement requires compensation for traversing the HRMA XRCF ARM glass substrate - systematics here could allow a common axial shift of both the HETG and LETG.

RC spacing		Focus to CAP CL	CAP CL to OTGorg	OTGorg to RC
mm	inches	inches	inches	inches
		(i) Drawing 301331:		
8772.83 mm	345.387	403.5	60.613	2.5
		(ii) Drawing 301331 with 0.392 shim:		
8782.79 mm	345.779	403.5	60.221	2.5
		(iii) Measurements with laser ranger:		
8787.99 mm	345.984	403.512	60.028	2.5

5.2.2 Rowland Spacing Mystery

X-ray measurements at XRCF, Section 6.2, have been used to verify the grating periods and Rowland spacing. Fits to the XRCF data using a Rowland spacing of 8788.04 mm (the mean of the HETG and LETG spacings of type (iii) above) show a discrepancy between the HEG/MEG sub-assembly periods and the X-ray derived periods; the results agree with the LETG subassembly period value. Because *both* the HEG and MEG periods appear in error by the same fraction, an HETG Rowland spacing error is a more simple explanation than coincident period errors. The Rowland spacing which agrees with the data is close to the expected design value given by case (ii) above. To minimize the number of Rowland spacing values kicking around, the current working hypothesis is that the HETG was installed at XRCF with a Rowland Spacing of 8782.8 mm. The origin of the difference between HETG and LETG XRCF Rowland spacings remains a mystery.

5.2.3 HETG Orientation at XRCF

The drawing of Figure 1.4 **when turned upside down** shows the HETG as oriented at XRCF. The view will then be from the HRMA towards the HETG with the +Z_facility (Up) at the top of the (flipped) page and +Y_facility (South) is to the right. This orientation is rotated 180 degrees about X from the Lab and Flight orientations.

Grating facet locations are given by a code such as 6EE3 where:

The leading digit is the shell number (1,3,4,6).

The next one or two letters specify the sector
(designated A, B,..., F, AA, BB,..., FF).
For the **XRCF orientation**:

sector A is between 9 and 8 o'clock
sector B is between 8 and 7 o'clock
...
sector F is between 4 and 3 o'clock
sector AA is between 3 and 2 o'clock
sector BB is between 2 and 1 o'clock
...
sector FF is between 10 and 9 o'clock.

The final number gives the grating location within
the sector (numbered 1,2,... increasing in CCW direction,
i.e., grating 1 is the most clockwise in a given sector.)

When used with the XRCF shutters the following HETG sectors are illuminated:

Shutter	Illuminated Sectors
Top	BB high-numbered half, CC, DD, EE low-numbered half
North	EE high-numbered half, FF, A, B low-numbered half
Bottom	B high-numbered half, C, D, E low-numbered half
South	E high-numbered half, F, AA, BB low-numbered half

5.3 Overview of HETG XRCF Measurements

5.3.1 Measurements and the CMDB

To support semi-automated test operation, the measurements to be made at XRCF were specified as rows in a 92 column tab-delimited ASCII file. These 92 columns specified nearly completely the desired state of the source, filters, HRMA, gratings, shutters, normalization detectors, and focal plane detectors. Testing proceeded through sequentially "executing" lines of this Calibration Measurement Data Base (CMDB). An as-run (or at least "as-requested"—modifications could be made manually in real time) version of the CMDB is now a useful starting point in understanding what data were taken.

Each measurement is labeled by a "TRW ID". The format of this label was created by TRW systems engineers (*e.g.*, the wild-man trio: Arenberg, Carlson, and Texter) as a convenient way to "name" the measurements. The format is given by:

`[Phase]-[Grating][FP Detector]-[Meas Type]-[Suite].[Number][char]`

Examples: `D-HXD-3D-11.020` or `H-HAS-EA-8.001`

where

`[Phase]` is the letter designation of the XRCF phase found in Table 5.2.

`[Grating]` indicates if a grating is inserted in the beam and takes on the values `I`, `H`, or `L` coresponding to the cases of no-grating, HETG, or LETG.

`[FP Detector]` indicates the focal plane detector through a two letter designation. The HXDA detectors (FPC, SSD, HSI) are specified by `XF`, `XS`, or `XH`; the ACIS-2C by `2C` and the ACIS and HRC detectors are specified with: `AI`, `AS`, `HI`, or `HS`.

`[Meas Type]` is a two character code used to indicate the general scientific purpose of the measurement being carried out. Valid types include `AL BG BU CR dF EA EE FA FC FM GI HF KF MC PI PO PW P1 P2 RC RF SC SF SG SL SM` and `3D` !

`[Suite]` is an integer used to group similar tests of a given type (a "suite" of tests).

`[Number]` is a three-digit integer to label a specific test within a suite.

`[char]` is an infrequent and optional additional character, *e.g.*, "`a`", to indicate a repeat of a measurement.

Tables 5.5 and 5.6 provide a summary of all data taken at XRCF with the HETG inserted in the optical path. The complete set of measurements is thus broken down by focal plane detector and measurement type. Reference to relevant sections of this report are given as well as the number of relevant measurements in brackets. These measurements, with hyper-links to CMDB summaries, are available on the web at:

`http://space.mit.edu/HETG/mtab/meas_table.html`

5.3.2 Efficiency Measurements

The measurement types related to effective area break into three main divisions based on source type: (*i*) quasi-monochromatic measurements using the EIPS sources: types EE (encircled energy), EA (effective area), and 3D(an automated version of EA); (*ii*) measurements using the DCM or HIREFS monochromators; and (*iii*) Molecular Contamination (MC) measurements where the broad-band continuum produced by the source is utilized, *e.g.*, Section 7.8).

The distinctions between EE, 3D, and EA are primarily in Phase 1 and represent different methods of placing the focal plane hardware at the desired location: in EE a beam-center is performed to set the aperture(s) precisely on the image center, using the starting location specified in the CMDB; in 3D measurements, one or more locations are sampled in the focal plane at coordinates specified by a locations file; and in EA the location is specified in the CMDB.

A valuable fraction of the data were taken using the XRCF monochromators, sometimes these were scanned in energy. These tests are all of type EA. Although scientifically similar to EIPS data, these data are more difficult to analyze because of the fundamental complication of the non-uniformity of the monochromators' beam. For scanned data there is the additional irritation that there was no direct synchronization between the source energy scan and the data collection.

In addition to these tests, the Alignment test was designed to set limits on vignetting due to (unplanned) decentering of the HETG at XRCF.

A large number of HETG-ACIS-2C data sets were taken that should allow grating-in/grating-out efficiency measurements to be made similar to the Phase 1 FPC/SSD measurements. These '2C analyses have not been carried out as of this writing, however.

In Phase 2, important effective area tests were carried out in the flight configuration, HRMA-HETG-ACIS-S, using the EIPS, monochromators, and continuum sources. Similar HRMA-HETG-HRC-I tests allow the untangling of grating and detector effects.

5.3.3 LRF Measurements

Phase 1 LRF measurements were generally performed with the HSI to obtain images. However, the FPC fitted with slits was used to scan the diffracted Mg-K line (PSF/1-D) and the beam center results of EE tests served to measure precisely the location of the diffracted images to determine grating periods and diffraction angles. The Alignment test performed on the MEG 3rd order was used to identify the specific mis-aligned gratings and in this context was a tool for LRF diagnosis.

Only a limited set of LRF related data were taken with the ACIS-S and HRC-I due to ACIS pileup (and hence time) limits, and HRC dose limits. The ACIS-2C LRF data is generally unanalyzed with the very notable exception of the scattering tests at 1.775 keV.

Table 5.5: Summary of HETG XRCF Measurements in Phase 1. The relevant report section is shown in **bold** and the number of measurements is shown in brackets.

Type	Detector	
	FPC/SSD	HSI
LRF-related . . . EE	Order locations: **6.2** [33]	-
FC, SF	-	Verify focus, check PSF, Mis-aligned gratings: **6.3**, **6.4** [16]
Alignment	-	Mis-aligned gratings: **6.4** [2]
dFocus	-	Defocus set of images: **N/A** [2]
PSF/1D	LRF core, wings: **6.3, 6.5** [21]	-
3D	-	MEG-Penning PSF: **6.3** [1]
PSF/Outer	-	Wings, scatter: **6.6** [8]
3D (Offaxis)	-	Offaxis images: **N/A** [6]
Eff.area-related . . . Alignment	-	Gross vignetting: **7.2** [1]
EE (EIPS)	Eff. area: **7.4** [*33*]	-
3D,EA (EIPS)	Eff. area: **7.4** [56]	Source spectra: **7.3** [32]
EA (MonoC)	Eff. area: **N/A** [29]	Source spectra (DCM, HIREFS): **7.3** [8]
3D (Molecular Contamination)	-	Identify and search for edges, etc.: **7.8** [6]

Table 5.6: Summary of HETG XRCF Measurements in Phase 2. The relevant report section is shown in **bold** and the number of measurements is shown in brackets.

Type	Detector		
	ACIS-2C	HRC-I	ACIS-S
LRF-related . . . FC, SF	Verify focus: **N/A** [7]	Verify focus: **TBD** [1]	Rowland geom.: **6.8** [2] Core, wings: **6.3** [1]
dFocus	Find best focus: **N/A** [10]	-	-
PSF/Inner	Core, wings: **N/A** [14] Offaxis images: **N/A** [9]	-	Offaxis images: **N/A** [4]
Scattering	Wings, scatter: **6.6** [5]	-	Grating scatter: **6.6** [6]
Eff.area-related . . . EA (EIPS)	Eff. area: **N/A** [126]	Eff. area: **7.9** [6]	Eff. area: **7.7** [7]
EA (MonoC)	Eff. area: **N/A** [36]	Eff. area: **7.9** [28]	Eff. area: **7.7** [15]
MC (Molecular Contamination)	Identify and search for edges, etc.: **N/A** [53]	- -	Identify and search for edges, etc.: **7.8** [5]

5.4 HETG-ACIS-S Data at XRCF

The measurements carried out at XRCF with the HETGS flight configuraion, HRMA-HETG-ACIS-S, are explicitly listed here because of their importance. This represents a diverse set of data both in terms of source/instrument modes as well as possibilities for analysis. References to the XRCF data analysis sections where the measurements are treated are given.

To-do:
Get actual defocus values for EA tests

Table 5.7: HETG-ACIS-S LRF Measurements at XRCF. All LRF measurements here were made with ACIS-S at nominal focus. All data are taken in TE mode unless noted.

TRW ID	run id	day	Source	Off-axis?	Comments
Rowland Geometry			EIPS:		Analysis Section 6.8
H-HAS-SF-1.001	115167	112	Al-K	-	scanned quadrants
H-HAS-SF-1.003	115168	112	Al-K	-	"
a.k.a. 'PI-1.001,3					
PSF Inner			EIPS:		Analysis Section 6.3
H-HAS-SF-18.001	115177-80	113	Al-K	-	TE alt. frame mode,
a.k.a. 'PI-18.001					scanned quadrants
Off-axis			EIPS:		
H-HAS-PI-1.011	115170	112	Al-K	0,3'	
H-HAS-PI-1.012	115171	112	Al-K	-4.2',-4.2'	
H-HAS-PI-19.001	115301	114	Si-K	-4.2',-4.2'	
H-HAS-PI-19.002	115302	114	Si-K	0,-10'	
Scattering			DCM:		Analysis Section 6.6
H-HAS-SC-7.001	115037	109	1.38	-	
H-HAS-SC-7.002	115038	109	1.38	-	
H-HAS-SC-7.003	115039	109	2.02	-	
H-HAS-SC-7.004	115040	109	2.02	-	
H-HAS-SC-7.005	115041	109	4-9	-	
H-HAS-SC-17.006	115113,4	111	4-9	-	TE alt. frame mode

Table 5.8: HETG-ACIS-S Effective Area Measurements at XRCF. All effective area measurements here are made on-axis. All data are taken in TE mode unless noted.

TRW ID	run id	day	Source	Defocus?	Comments
Effective Area			EIPS:		Analysis Section 7.7
H-HAS-EA-2.001	115169	112	Al-K		
H-HAS-EA-6.001	115310	114	O-K		
H-HAS-EA-6.002	115443,4	115	Fe-L		TE alt. frame mode
H-HAS-EA-6.003	115373	115	Cu-L		TE alt. frame mode
H-HAS-EA-6.004	115303	114	Si-K		
H-HAS-EA-6.005	115451	115	Fe-K		TE alt. frame mode
H-HAS-EA-6.006	115366	115	Cu-K		TE alt. frame mode
Effective Area			DCM:		Analysis Section 7.7
H-HAS-EA-8.001	115026	109	0.95-1.15		
H-HAS-EA-8.002	115027	109	1.2-1.4		
H-HAS-EA-8.003	115028	109	1.4-1.7		
H-HAS-EA-8.004	115029	109	1.86-2.00		
H-HAS-EA-8.005	115030	109	2.05-2.35		
H-HAS-EA-8.006	115032	109	2.5-4		
H-HAS-EA-8.007	115033	109	4-5		
H-HAS-EA-8.008	115034	109	5-7		
H-HAS-EA-8.009	115035	109	7.2-8.7		
Effective Area			HIREFS:		Analysis Section 7.7
H-HAS-EA-10.001	115488	116	0.392		
H-HAS-EA-10.002	115489	116	0.486		
H-HAS-EA-10.003	115490	116	0.577		
H-HAS-EA-10.004	115491	116	0.642		
H-HAS-EA-10.005	115492	116	0.751		
H-HAS-EA-10.006	115493	116	0.800		
Molecular Contamination			EIPS:		Analysis Section 7.8
H-HAS-MC-3.001	115360	115	Cu	0.0	CC mode, HEG only
H-HAS-MC-3.005	115362	115	Cu	0.0	CC mode, MEG only
H-HAS-MC-3.010	115264	113	C	0.0	CC mode, HEG only
H-HAS-MC-3.011	115265	114	C	0.0	CC mode, MEG only
H-HAS-MC-20.001	115359	115	Cu	0.0	TE alt. frame mode

5.5 Examples of XRCF Data

With complicated data it is best to start with an image—and so in Phase 1 we generally took images of the diffracted X-rays with the High Speed Imager (HSI). Figure 5.3 shows the HSI image of the Al-K line in the MEG 3rd order—deflected 55 mm from the zero-order (HRMA focus) location. These are the "raw" HSI data and show the instrumental "gaps"[21], *e.g.*, one goes through the K-β peak. Note that the "line" in fact consists of several discrete lines as well as continuum. The "satellite" line just shortward of the K-α peak has been previously observed during XMM grating testing[60]; we also observe a second, weaker satellite line at 8.22Å.

To accurately measure the intensity of the line in Phase 1, the FPC_X2 (or SSD_X) with selected aperture could be moved to the line center and the pulse-height histogram of events through the aperture measured. An example of the acquired focal-plane and BND histograms is shown in Figure 5.4 for the MEG first order of Al-K and a 500 μm diameter aperture. Note that while the BNDs are able to resolve an Al-K peak and broadband continuum, the detailed spectral structure of the Al-K line is unresolved. The 500 μm first-order aperture size corresponds spectrally to the region within the 1500 μm circle shown in Figure 5.3—thus the FPC_X2 is detecting the K-α and satellite lines and some continuum, but is excluding other continuun and the K-β peak.

In Phase 2 the focal plane detectors were all imaging instruments (ACIS-2C, ACIS, and HRC) and so provide their own source spectral diagnostics. Effective area measurements generally did not required precise positioning; in fact, because of per-pixel count-rate limits (set generally by pile-up for ACIS and dose limits for HRC) the measurements were performed with a large defocus. Figure 5.5 shows an ACIS-2C image of the HEG first-order of Al-K. The defocussed images of the HRMA shells 4 and 6 are modulated by the individual grating facets. Because of the defocus, extraction of the K-α events will necessarily be contaminated by the existence of the other lines and continuum. HRC and ACIS effective area data are very similar to this ACIS-2C example as the ACIS-S event plot of Figure 5.6 demonstrates.

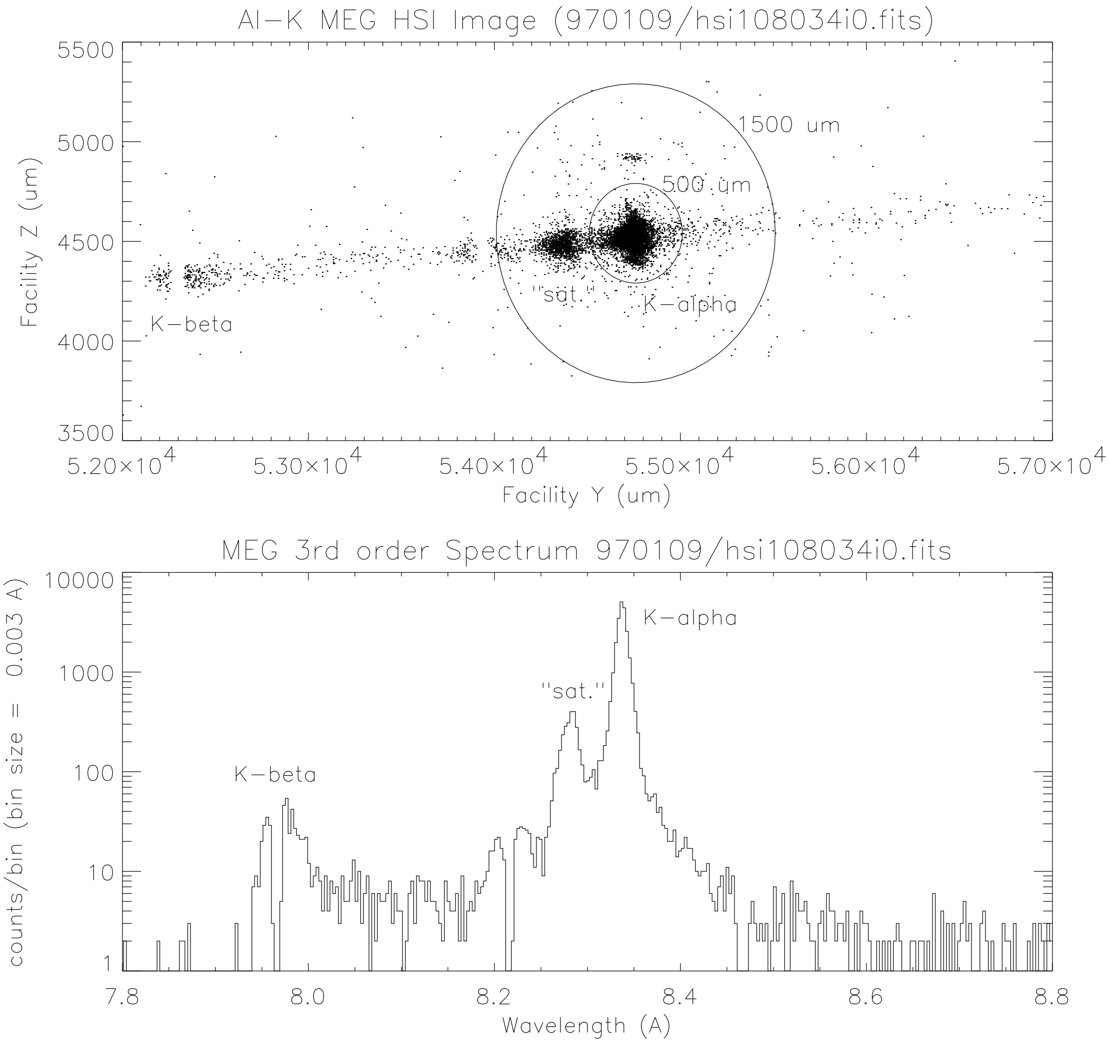

Figure 5.3: HSI image of 3rd-order MEG Al-K line (top) and the resulting grating-produced spectrum (bottom). Note that all of this spectral structure is unresolved by the FPC and SSD detectors, Figure 5.4. A strong "satellite" line is clearly visible near the K-α peak. HSI instrumental gaps have not been removed, *e.g.*, at the K-β line.

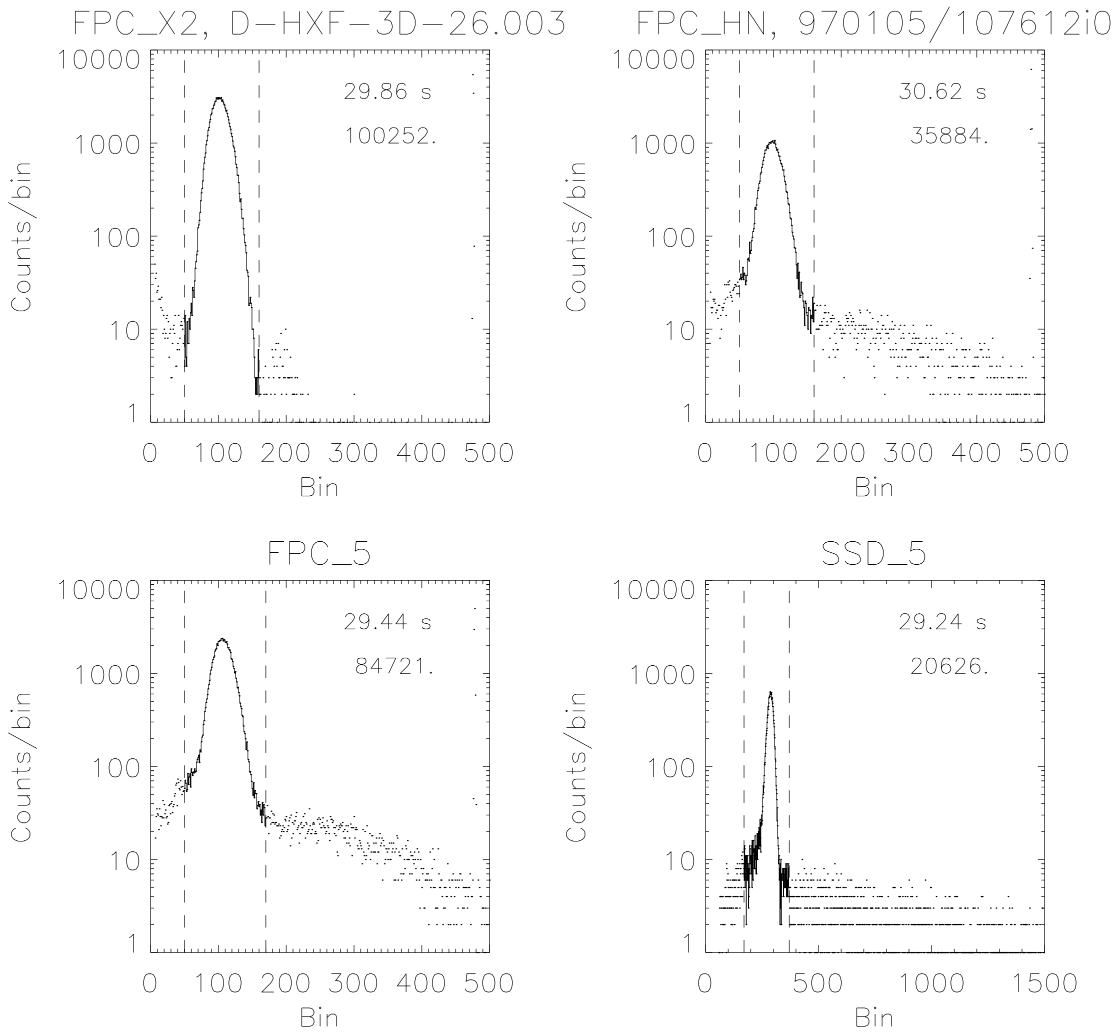

Figure 5.4: PHA spectra from Al-K MEG +1 order measurement. The focal plane FPC_X2 shows only a monochromatic response (with a slight pile-up peak at $2E$) while the beam normalization detectors (FPC_HN, FPC_5, and SSD_5) show both the Al-K "line" and broad-band (unfiltered) continuum.

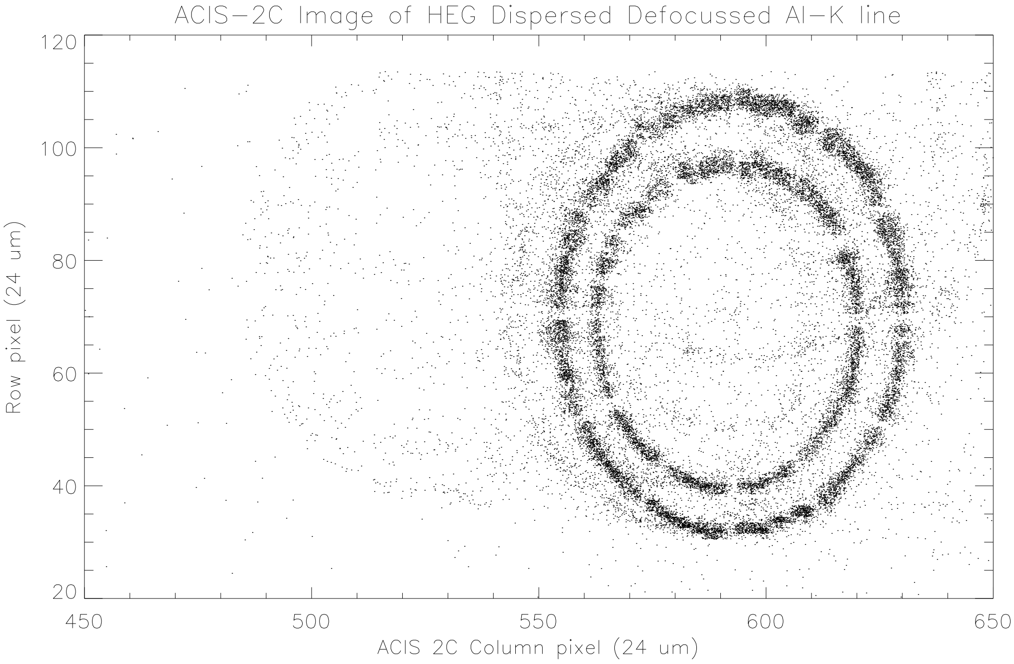

Figure 5.5: ACIS-2C defocussed image of HEG dispersed Al-K line. Note that the same line components as in Figure 5.3 are present.

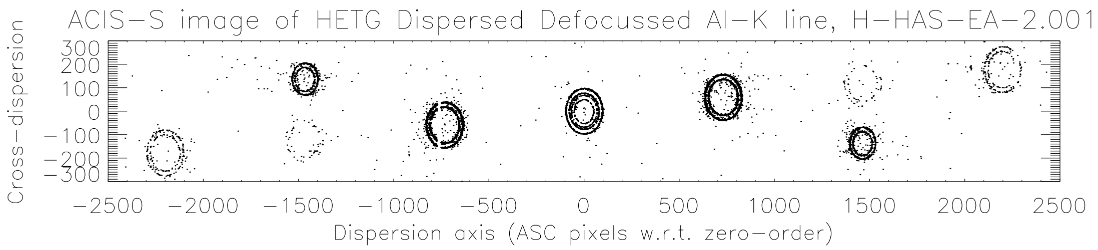

Figure 5.6: ACIS-S defocussed image of HETG dispersed Al-K line. The HEG and MEG diffracted orders are clearly identified by the corresponding HRMA shells in their images. For the MEG, orders $m = \pm 1, \pm 2, \pm 3$ are visible.

5.6 Status of the HETG XRCF Analysis

The table below summarizes the status of the HETG XRCF analysis efforts. Only a few of the measurement projects listed here have reached the level of "adequate" analysis. Analysts are generally from the HETG and ASC/MIT groups; brackets indicate contributors expected beyond this preliminary report.

Table 5.9: Analysis Status Code

Status code	Analysis status
-	not yet analyzed
X	very preliminary analysis
XX	adequate analysis
XXX	complete analysis

Table 5.10: Status of HETG XRCF analyses

Section	Analysis Effort	Prime Analyst	Status
	LRF:		
6.2	Periods and Angles	Dewey	XX
6.3	Core: Period and Roll Variations	Dewey	XX
6.4	MEG mis-aligned gratings	Dewey	XXx
6.5	Between Core and Scatter	Dewey	x
6.6	Scatter Tests	Marshall	XXX
3.3	Scatter Theory	J.Davis	XXx
6.7	Offaxis and Defocus Tests	-	-
6.8	ACIS-S Rowland Conformance	Stage	XXX
	Efficiency and Effective Area:		
7.2	Alignment Tests	Dewey	X
7.3	XRCF Source Characteristics	Dewey	XXX
7.4	Phase 1, EIPS Data	Dewey	XXx
7.5	Phase 1, Monochromator Data	-	-
7.6	Efficiency with ACIS-2C Data	-	-
7.7	Area with ACIS-S	Schulz	XXx
7.8	Molecular Contamination	Marshall	XXx
7.9	Area with HRC-I	Flanagan	XX
7.10	High-Order Efficiencies	Flanagan	XX